

Investigation of a cohesive granular material: multi-scale modelling by FEM-DEM approach

Trung Kien NGUYEN¹, Gaël COMBE¹, Denis CAILLERIE¹, Jacques DESRUES¹

¹UJF-Grenoble 1, Grenoble-INP, CNRS UMR5521, 3SR Lab., B.P.53, 38041 Grenoble Cedex 09, France, e-mail: trungkien.nguyen@3sr-grenoble.fr

Abstract

This article presents the multi-scale modelling of cohesive granular materials, its numerical implementation and its interesting results. At microscopic level, a Discrete Element Method (DEM) is used to model dense grains packing. At the macroscopic level, the numerical solution is obtained by the Finite Element Method (FEM). In order to bridge the micro and macro scales, the concept of Representative Elementary Volume (REV) is applied, in which the average REV stress and the consistent tangent operators are obtained in each macroscopic integration point as the results of DEM's simulation. In this way, the numerical constitutive law is determined through the detailed modelling of the microstructure, and taken into account the nature of granular materials. We first elaborate the principle of the computation homogenization (FEMxDEM) and then demonstrate the features of our multi-scale computation in terms of a biaxial compression test. Strain localization is observed and discussed.

Key words: Multi-scale, FEM, DEM, homogenization, cohesive granular materials.

1. INTRODUCTION

Numerical modelling is widely used to investigate and design the resistance of buildings or geotechnical problems. Classically, Finite Element Method (FEM) (Zienkiewicz [1]), which is based on a continuum approach, is applied. This method is appropriate for a wide range of applications (soil mechanics, structures, concrete, ...). However, earth structures specifically made of granular materials are very common (Chevalier *et al.* [2]). These materials are discontinuous and heterogeneous by nature. They generate many complex mechanical responses when they are subjected to large deformations (Lanier [3]). Unfortunately, it is difficult to realistically model the discrete nature of granular media by FEM. It is not the case for the Discrete Element Methods (DEM) that has been especially developed to model the granular matter at the grain scale. This specific method consists in the integration of the equations of motion to obtain the response of an assembly of rigid particles (Cundall [4]). Thus, the granular media is modelled at the contact scale and their discrete nature can be captured.

It is widely known that the macroscopic behaviours take its origins at the grain scale (inter-granular contact behaviour, contact network, density, ...) hereafter called the *microstructure*. The mathematical and the numerical description of a multi-scale relationship between the microstructure and the macroscopic mechanical behaviour is an essential issue. Recently, several authors have proposed multi-scale approach (Kouznetsova *et al.* [5, 6], Miehe and Dettmar [7, 8], Meier *et al.* [9]) to investigate the overall behaviour of heterogeneous materials using mechanical informations from the microstructure. Thus, the materials are studied at two different scales.

In this paper, we propose a multi-scale numerical homogenization approach by combining FEM and DEM to study the behaviour of cohesive granular materials. The microstructure of the granular soil is thus modelled by using the DEM approach on a Representative Elementary Volume (REV) made of few grains. At the large scale (sample scale), the FEM approach is used. The idea of coupling FEM and DEM emerged in the late 1980's with the great advancement in computational power (Munjiza *et al.* [10]). Other contributions should also be noticed (Munjiza [11], Oñate and Rojek [12], Wellmann

and Wriggers [13]). In these works, FEM is used to model zones in which small deformations occurs whereas zones with large deformation are handled with the DEM approach. The coupling between these two zones involves interacting contact domain.

In our work, the coupling between the FEM and the DEM is different. Whereas the overall earth structure is modelled by a FEM approach, the constitutive mechanical behaviour used at each Gauss points of the mesh does not come from a mathematical phenomenological law but from a numerical behaviour computed with DEM of a REV. The micro (DEM) and the macro (FEM) scales are thus bridged by a homogenisation process.

In fact, due to the coefficient of friction, the behaviour of granular media is not elastic and is strain history dependent which means that the stress at some instant depend not only on the strain at that moment but on the whole history of strain up to it. The boundary value problems (BVP) involving solids presenting such a behaviour are therefore evolution problems. Very often, those evolutions are slow enough so that inertial effects can be neglected and the evolution is quasi-static which means that at any time the medium is balanced. The numerical resolution of this type of problem is usually performed using a time stepping discretisation. In this method, the equilibrium equations are written at each time step, and the constitutive law is integrated through a specific method adapted to the law (see for instance Simo and Hughes [14] for elastoplasticity). That yields an "integrated" constitutive equation: $\epsilon_n \rightarrow \sigma_n$ giving the stress at the end of the step n in terms of the strain at the end of the same step and therefore looking like an elastic, generally non linear, constitutive equation.

The problem to be solved at time step n is a nonlinear elastic-like equilibrium problem, generally solved using the Newton's method. The standard Newton's method requires the differentiation of the integrated law which leads to the notion of consistent tangent operator (for elastoplasticity, see Simo and Hughes [14])

In the FEM \times DEM approach, the macroscopic constitutive equation of the equivalent continuous granular medium is obtained through the DEM simulation of the motion of the grains in a REV subjected to a history of macroscopic strain. The integrated law of each time step is then directly the constitutive equation of the continuous medium for a macroscopic strain path completely determined by the strain at the end of the step. In this case, the numerical differentiation, which seems to be the only way to get the consistent tangent operator of the the integrated law on a time step, poses problems, a variant of Newton's method is used, either by keeping the linear operator of all the time step and all the iterations equal to the elastic one of initial REV or computing at each iteration of the Newton's method of a given time step the homogenized linear elastic constitutive equation of the current REV the set of contacts between grains of which has been fixed.

The paper is organized as follows. Section 2 presents the homogenization methods to bridge the scale between micro- and macro- level. Section 3 describes the numerical model by DEM. Some numerical results done with the multi-scale computation (FEM \times DEM) is demonstrated in section 4.

2. HOMOGENIZATION METHOD

Following the explanations given above, a quasi-static finite strain continuum formulation is considered at the macroscopic level. The constitutive response at this level is obtained from DEM computations on a Representative Elementary Volume (REV). The displacement gradient for a macroscopic Gauss point is imposed on the REV associated to this point. The Cauchy stress can be computed in using a well established homogenization formula (eq. (1)) (Weber [15]). The upscaling technique consists of using DEM model at each Gauss point of the FEM mesh to derive numerically a constitutive response. This framework is illustrated in figure 1.

For a given history of a macroscopic displacement gradient $h_{kl} = \partial u_k / \partial x_l$, the macroscopic Cauchy stress σ_{ij} results from microscopic forces between grains through a homogenization formula (eq. (1)).

$$\sigma_{ij} = \frac{1}{S} \cdot \sum_{(n,m) \in C} \vec{f}^{m/n} \otimes \vec{r}^{nm} \quad (1)$$

Where S in 2D case is the area of the microstructure; f_i^c and l_j^c are respectively the component i of

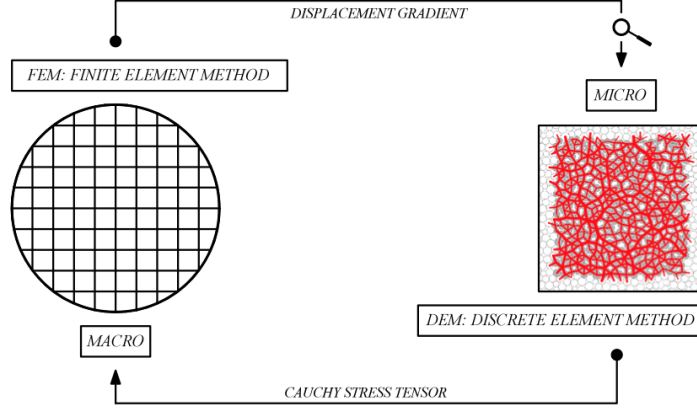


Fig. 1. Computational homogenization scheme

the contact forces acting in contact c and the component j of the branch vector l joining the mass centre of two grains in contact.

The numerical procedure allows us to build the constitutive law of the form (eq. (2)) that expresses the stress as a function of the history of displacement gradient.

$$\boldsymbol{\sigma}(t) = \Gamma^t \{ \mathbf{h}(\tau), \tau \in (0, t) \} \quad (2)$$

For a given displacement gradient h_{kl} , we can construct the tangent stiffness matrix:

$$C_{ijkl} = \frac{d\sigma_{ij}}{dh_{kl}} \quad (3)$$

Eq. (3) gives the definition of the tangent stiffness matrix. In finite deformation analysis, the stress response requires solving a nonlinear system of equations when the mechanical behaviour is nonlinear, which is the case for granular materials. In order to solve the non-linear system of equations, an incremental-iterative strategy Newton-Raphson method is adopted. This requires the implementation of a consistent tangent matrix in the numerical integration scheme. Then, the consistent tangent operators computed from the stress state at the end of the load step are consistent with the algorithm of integration used. Any inconsistency between the tangent operator and the algorithm of integration of the constitutive law will spoil the quadratic convergence of the Newton-Raphson method. Moreover, the more this operator represents the mechanical behaviour of granular media, the faster the iterative process converges to the solution.

The consistent tangent operators can be found analytically for the simple law, but for the other complex laws, a numerical differentiation has to be adopted.

At the macroscopic scale, finite elements are employed to solve the homogenized problem. When an incremental linearization procedure is adopted, the matrix (eq. (3)) should be evaluated numerically. We describe here this numerical procedure: the tangent stiffness is computed in two steps.

For an increment of displacement gradient δh_{kl} , we perform a first step in which we compute the stress at the end of this increment, noted $\sigma_{ij}(\delta h_{kl})$. Then we consider perturbed increments of displacement gradient $\delta h_{kl} + \varepsilon \cdot \Delta_{kl}^{mn}$. Here ε is a small parameter and Δ_{kl}^{mn} is a second-order tensor such that its components are defined as:

$$\Delta_{kl}^{mn} = \delta_{mk} \cdot \delta_{nl} \quad (4)$$

with the Kronecker symbol $\delta_{mk} = \begin{cases} 1 & \text{If } m = k \\ 0 & \text{If } m \neq k \end{cases}$. In two-dimensional case: $k, l, m, n = 1, 2$.

Finally, the results of these two steps allow for the determination of consistent tangent operator:

$$C_{ijkl} = \frac{\sigma_{ij}(\delta h_{kl} + \varepsilon \cdot \Delta_{kl}^{mm}) - \sigma_{ij}(\delta h_{kl})}{\varepsilon} \quad (5)$$

This procedure is performed in every time step and in every Gauss point of the macroscopic finite element discretization. At the beginning and the end of each step, the REV is in a state of equilibrium.

3. MICROSCOPIC DEM MODEL

The numerical model of granular material behaviour is herein obtained by a classical discrete element approach (DEM with soft-contact dynamics type) using bi-Periodic Boundary Conditions (PBC). (For details see Radjai and Dubois [16]). A Representative Elementary Volume (REV) is associated at each Gauss point. This REV is made of a dense packing of 400 2D polydisperse circular particles. All grains interact via linear elastic laws and coulomb friction when they are in contact. Accordingly, the normal repulsive contact force f_{el} is related to the normal apparent interpenetration δ in the contact as $f_{el} = -k_n \cdot \delta$, where k_n is a normal stiffness coefficient ($\delta < 0$ if a contact is present, $\delta = 0$ if there is no contact). In order to model a cohesive materials, a local cohesion is introduced at the level of each pair of particles by adding an attractive force f_c to f_{el} ; f_c is constant for each contact. Thus, the overall normal force for two grains in contact is $f_n = f_{el} + f_c$. The Coulomb inequality $|f_t| \leq \mu \cdot f_{el}$ requires an incremental evaluation of f_t in each time step ($\Delta f_t = k_t \cdot \Delta u_t$, where Δu_t is the tangential relative displacement in the contact and k_t is the corresponding tangential stiffness), which leads to some amount of slip each time one of the equalities $f_t = \pm \mu \cdot f_{el}$ is imposed (Cundall [4]). In the present study, k_n is such that $\kappa = k_n/\sigma_0 = 1000$ (Combe et Roux [17]), where σ_0 is the 2D isotropic pressure. The stiffness ratio is arbitrary fixed to $k_n/k_t = 1$. The cohesive force f_c should be defined with reference to the mean level of pressure as suggested by Gilibert *et al.* [18], Radjai and Dubois [16]: $p^* = f_c/(a \cdot \sigma_0)$ where a is typical diameter of grains. So p^* is a ratio measuring the attractive part of a contact force versus the repulsive part due to particle interpenetration. Hereafter $p^* = 1$. The inter-granular angle of friction is $\mu = 0.5$.

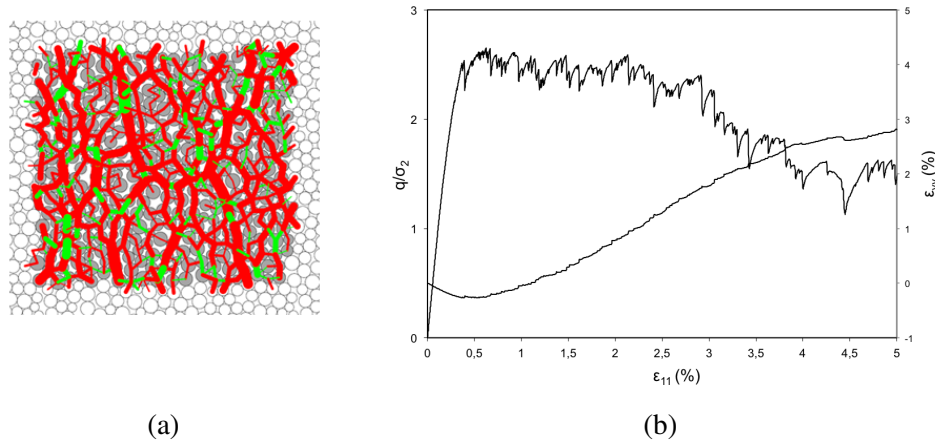


Fig. 2. Biaxial by DEM on a REV contains 400 particles with PBC: (a) REV deformed. Contact forces are displayed with the convention: the width of the lines joining the centres of two particles in contact is proportional to the normal force. Red, green line distinguish respectively ($f_c \neq 0$) and ($f_c = 0$). (b) Macroscopic response.

A degradation of the cohesion can be taken into account by considering a reduction or vanishing of f_c in a contact when sliding or separation occurs. Here we consider the second case (vanishing cohesion), which corresponds approximatively to a material with brittle cemented contacts.

The figure 2(a) shows an assembly of 400 particles submitted to a deviatoric loading (vertical compre-

ssion test with constant lateral stress - hereafter called *biaxial test*). The stress-strain response is displayed on the Fig 2(b). Because this REV is initially dense, the volumetric strain is therefore essentially dilative

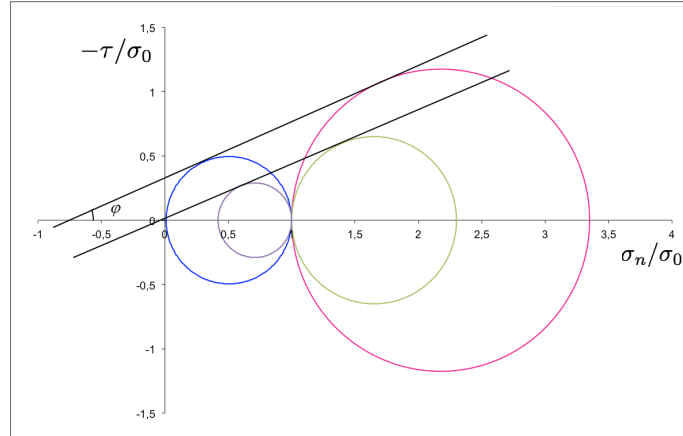


Fig. 3. Mohr-Coulomb criterion. Mohr circles are plotted with color conventions: biaxial compression at peak (in rose), post peak (in green); biaxial extension test at peak (in blue), post peak (in violet).

The Mohr-Coulomb criterion is widely applied for cohesive granular materials. This model characterizes the mechanical strength of materials in two parameters: a macroscopic cohesion parameter C and an internal friction angle ϕ . These parameters can be determined from different tests, such as shear, compression or extension tests. Here we consider two biaxial tests: one in compression and the other in extension path. Mohr circles are drawn and plotted in the figure 3. The yield surface in the stress plane of materials is described. As shown on this figure, two parameters are determined at different states which characterize the material's strength at particular moments such as peak stress and post-peak (for large vertical strains) when the degradation of cohesion is observed at almost all contacts. At peak stress, from the circles, we can obtain $\phi = 25^\circ$ and $C/\sigma_0 = 0.3$. The circles at post-peak points show clearly the vanishing of macroscopic cohesion when the local contact cohesion is lost but the internal angle of friction remains the same. The internal angle of friction is 25° .

4. MULTISCALE FEM \times DEM SIMULATION

The FEM \times DEM approach was implemented in the FEM code Lagamine (Charlier [19]) which is able to manage large strains. The implementation involved significant modification in the original code, but it essentially consisted in adding the DEM modelling as a constitutive numerical law.

Biaxial experimental tests have been performed in Grenoble for a long time (Desrues [20]). Many test results are presented in the overview paper by Desrues and Viggiani [21]. The principle of the test named *shf03*, lubricated at two surfaces and showing two symmetric shear bands is now chosen to be modelled by our multi-scale tool. Using the symmetry, only one-fourth of the test specimen is modelled. This test is carried out in two steps: isotropic compression until $\sigma_1 = \sigma_2 = \sigma_0$ and then loading on the upper surface to reach the desired axial deformation. During the axial loading, the lateral pressure is kept constant and equals $\sigma_2 = \sigma_0$. (For more details about the experimental setup, we refer the readers to Desrues and Viggiani [21]).

The initial FE mesh of the problem and the boundary conditions are systematically given in the figure 4. The mechanical problem is discretized spatially using elements Q8 (8 nodes per element). The number of integration Gauss points is chosen as 4 for each element (Fig. 5 left). This choice is to work with a degree of interpolation less strictly than the number of the nodes, in order to improve the convergence of the numerical scheme and avoid locking a problem due to the spatial discretization. In this study, three different types of mesh with the same boundary conditions are used. The first and the second are structural meshes, which consist of 128 elements, and 64 elements Q8. The last one is a non-structural

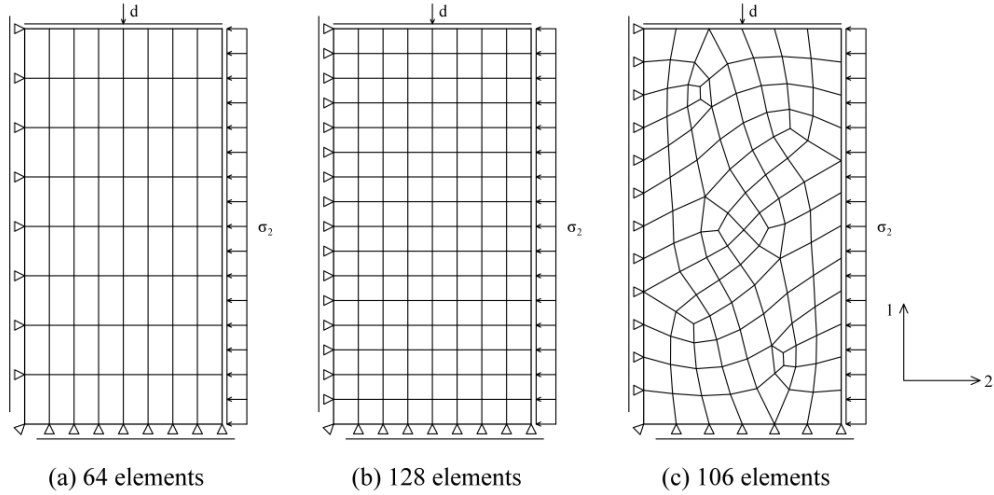


Fig. 4. Spatial discretization by FE at macro-scale: (a,b) structural mesh and (c) non-structural mesh.

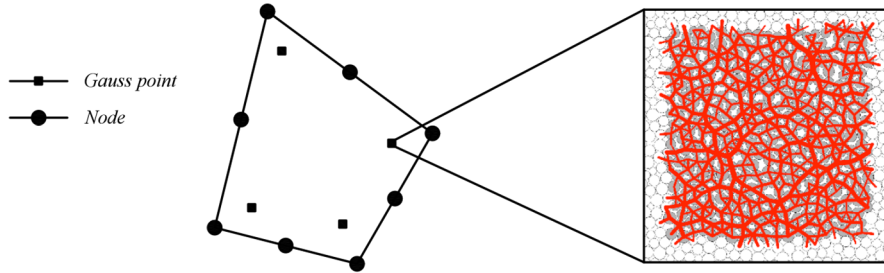


Fig. 5. Element Q8 and REV initially similar at each Gauss point.

mesh of 106 elements Q8 (Fig. 4). At micro-scale, a REV of 400 particles, initially similar, is used at each gauss point. At the initial state, the cohesive force exist at all the contacts (which is represented by a red line joining the centres of two grains in contact) (Fig. 5 right).

4.1. Macroscopic results

The simulated behaviour via the FEM \times DEM approach is shown on the figure 6(a) while the right figure (Fig. 6(b)) gives the comparison between our methods and the results come from DEM simulation on a single cell with PBC. This figure presents the deviatoric stress $q = \sigma_1 - \sigma_2$ as a function of axial deformation ϵ_{11} . The first remark is that this mechanical behaviour is typical of what is classically observed on a laboratory drained triaxial test on dense cemented sands, or weak sandstones: from the isotropic state, the specimen is first deformed homogeneously; meanwhile, the deviatoric stress $q = \sigma_1 - \sigma_2$ increases until it reaches a peak corresponding to the maximum strength of the materials. Then, one can observe a softening behaviour (stress drops down) until $q = \sigma_1 - \sigma_2$ reach a plateau. Concerning the response of the DEM's simulation: as the number of particles increases, the macroscopic response bends generally to a final solution (from blue (400 particles) to green (22500 particles) and orange (40000 particles) curve in the figure 6(b)). But in fact, we cannot obtain the FEMxDEM response with this type of simulation. In addition, we observe that the solutions by different meshes (by FEM \times DEM) is not unique after the peak (Fig. 6a).

The softening (post-peak response of the specimen) is more pronounced if compared with purely frictional models (not shown here), for two reasons: one is that the degradation of the cohesion comes in

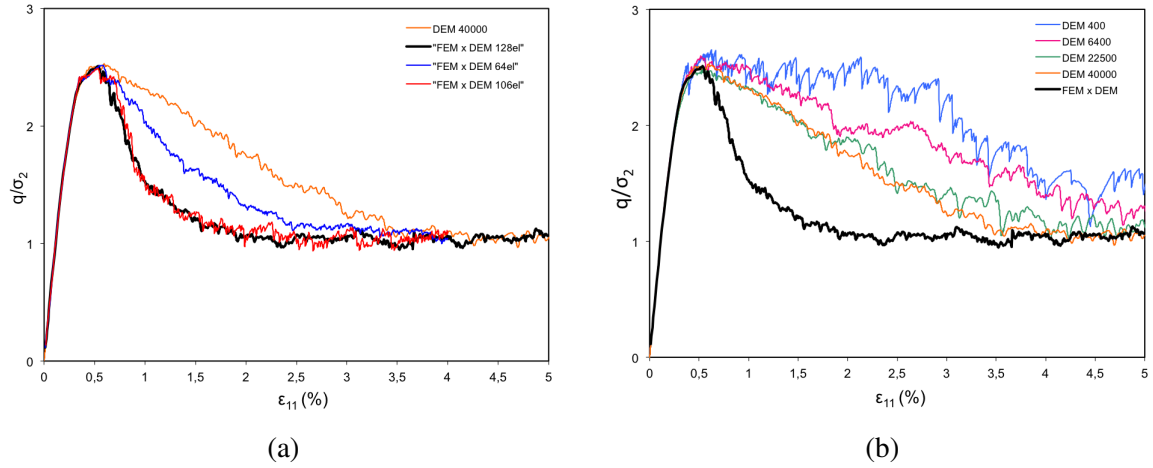


Fig. 6. Macroscopic response of multi-scale FEM \times DEM computation. Comparison between FEM \times DEM and DEM methods using different levels of discretization for FEM and DEM: (a) DEM model with 40000 particles versus multiscale model with different numbers of elements; (b) multiscale model with 128 elements versus DEM models with different numbers of particles.

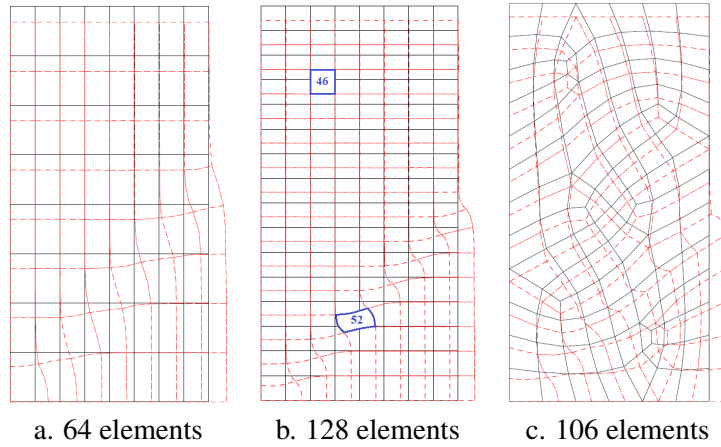


Fig. 7. Deformed of structure at $\epsilon_{11} = 3\%$.

addition to the other degradation mechanisms like dilatancy and changes in contact orientation distribution; the second reason is strain localization. Around a peak stress, the strain suddenly localizes into shear band. It is well known in FEM modelling that softening constitutive models lead to localization in the response of the boundary value problems (BVP). In experimental tests, localization occurs as well (Desrues and Viggiani [21]), and the seek for a proper modelling of strain localization has been a crucial research objective for three decades now.

We observe here, not surprisingly, that localization occurs as well in the multi-scale FEM \times DEM approach. In the figure 7, the local distortion of the mesh shows clearly a shear band in the specimen, confirmed on the figure 8 by the map of the second invariant of the deviatoric strain. Due to strain localization, deformation is observed to concentrate in this narrow zones (called *shear band*) (Desrues and Chambon [22]); a given increment of top boundary displacement is no more accommodated by an overall strain in the whole specimen, but by a much faster shear deformation process in the band. This is the reason for a much faster softening of the specimen response than the REV response.

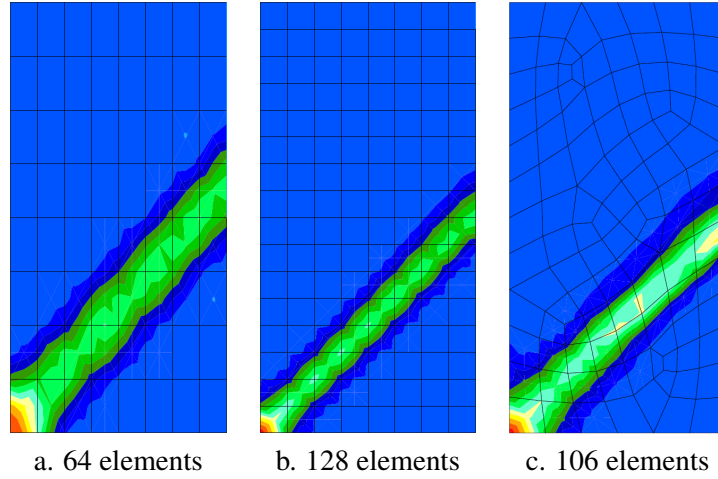


Fig. 8. Second invariant of strain tensor at $\epsilon_{11} = 3\%$.

4.2. Microscopic analysis

In order to highlight the advantage of our methods and to understand the origin of macroscopic phenomena, which comes from microscopic evolution, in this section, we propose to analyze the stress evolution in various Gauss points at different location in the mesh. The mesh of 128 elements Q8 is chosen for this analysis. The focus is on the Gauss points into Q8 n^o 46 and Q8 n^o 52 (see Fig. 7b). The element 52 is in the shear band whereas the element 46 is far from the shear band, in a homogeneous zone.

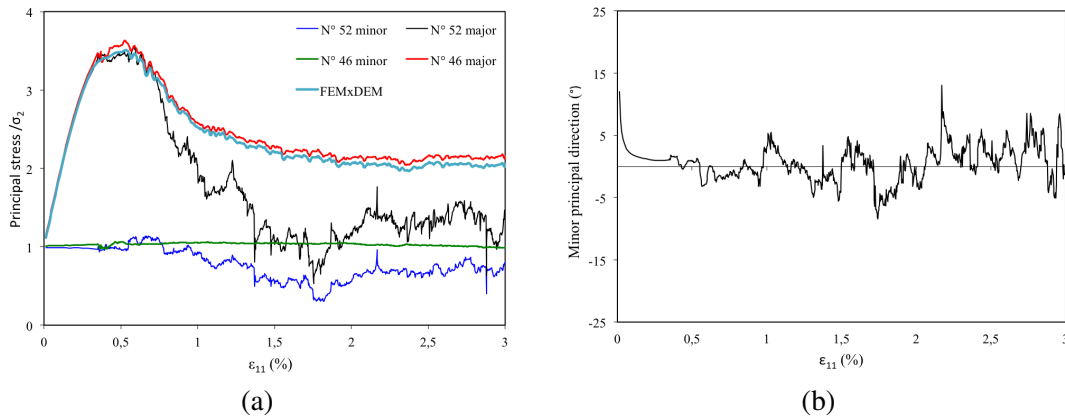


Fig. 9. Microscopic analysis: (a) Principal stress in elements 46 and 52. (b) Principal direction in element 52. ϵ_{11} is the equivalent overall axial strain for the specimen.

Figure 9a shows the evolution of principal stresses (PS hereafter) (minor and major) in the two elements. As for the major PS, we observe that their respective evolutions diverge once the maximum shear strength is reached. The stress variations are rather smooth in element 46 and noisy in 52. Both 46 and 52 show stress reduction, which is consistent with the softening of the specimen as a structure: despite the degradation of the material's properties is concentrated in the shear band, it results in a fall of stress in the whole specimen as soon as the band becomes the overall failure mechanism. The minor PS shows the same trend with respect to smoothness. Within the shear band, not only PS values but also PS directions (Fig. 9(b)) show erratic values. Clearly, the shear band becomes the only active part of the specimen once localization has started; in this active zone, the deformation process is intensive and

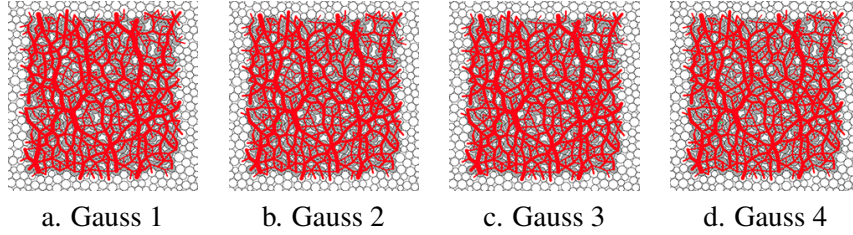


Fig. 10. REV deformed at Gauss point of element 46 $\epsilon_{11} = 3\%$. (See Fig. 2 for color convention).

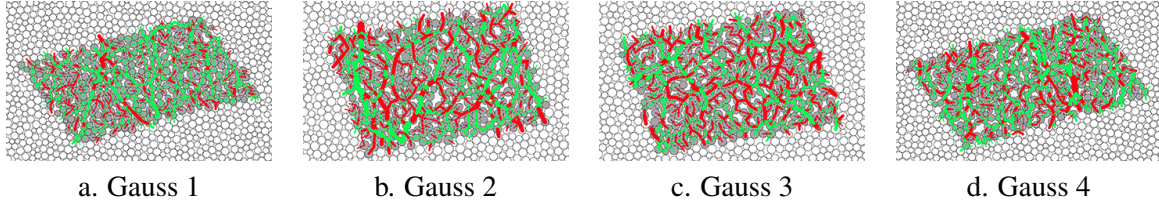


Fig. 11. REV deformed at Gauss point of element 52 at $\epsilon_{11} = 3\%$. (See Fig. 2 for color convention).

produces large micro-structural reorganization with severe scattering in the local stress.

In figures 10 and 11, the REV at deformed state are plotted. All the Gauss point have the same initial configuration (Fig. 5) but the deformed configurations becomes quite different at the end. All the REV at element 46 remain similar to the initial state with only one or two contact losing cohesion, while the REV at element 52 is subjected to a complex loading at each REV (both compression and shear loading, see the shape of REV) while a degradation of cohesion forces is observed throughout these REV (contacts without cohesion are illustrated by the green line). We can conclude that in the shear band zone, the strain localization leads to a generalized inter-granular cracking.

5. CONCLUSIONS

A two-scale approach to investigate the behaviour of cohesive granular materials has been presented, combining DEM at the micro level with FEM modelling at macroscopic level. A numerical homogenization method is considered to bridge the gap between different scales. At small scale level, kinematics condition is applied at each REV with PBC. The mean stress is recovered together with the consistent tangent operators to construct the macroscopic constitutive law. This new method allows us to obtain the overall behaviour of geomaterials together with the micro mechanism inside REV at every point in the FEM mesh. The DEM code is successfully implemented in a large strain finite elements code Lagamine. Using this numerical tool, some results from biaxial test simulation were presented and analyzed. Strain localization has been observed. The mechanical response of cohesive granular materials was investigated both at the macro- and microscopic level. Moreover, local stress evolutions, the inter-granular cracking at micro level (REV cell) have been highlighted to understand the origin of the macroscopic behaviour.

Acknowledgments. This work was carried out as a part of GeoBridge project research at 3SR Lab, Grenoble, France. The authors would like to thank the French National Agency of Research (ANR - Agence Nationale de la Recherche) for this support.

REFERENCES

- [1] Zienkiewicz, O.C. (1979), La méthode des éléments finis, *Mc Graw-Hill Inc.*
- [2] Chevalier, B., Villard, P., Combe, G. (2011), Investigation of load-transfer mechanisms in geotechnical earth structures with thin fill platforms reinforced by rigid inclusions, *International Journal of Geomechanics* **11(3)**, 239-250.
- [3] Lanier, J. (2001), Mécanique des milieux granulaires, *Hermes science publications.*
- [4] Cundall, P.A. and Strack, O.D.L. (1979), A discrete numerical model for granular assemblies, *Geotechnique* **29(1)**, 47-65.
- [5] Kouznetsova, V., W.A.M. Brekelmans and F.P.T. Baaijens (2001), An approach to micro-macro modelling of heterogeneous materials, *Computational Mechanics* **27**, 37-48.
- [6] Kouznetsova, V., M.D.G. Geers and W.A.M. Brekelmans (2002), Multiscale constitutive modelling of heterogeneous materials with a gradient-enhanced computational homogenization scheme, *Int. J. Numer. Meth. Engr.* **54**, 1235-1260.
- [7] Miehe, C. and J. Dettmar (2003), A framework for micro-macro transitions in periodic particle aggregates of granular materials, *Comput. Methods Appl. Mech. Engrg.* **196**, 225-256.
- [8] Miehe, C., J. Dettmar and D. Zah (2010), Homogenization and two-scale simulations of granular materials for different microstructural constraints, *Int. J. Numer. Meth. Engr.* **83**, 1206-1236.
- [9] Meier, H.A., P. Steinmann and E. Kuhl (2007), Towards multiscale computation of confined granular media, *Technische Mechanik* **28(1)**, 32-42.
- [10] Munjiza, A., D.R.J. Owen and N. Bicanic (1995), A combined finite-discrete element method in transient dynamics of fracturing solids, *Engineering Computations* **12(2)**, 145-174.
- [11] Munjiza (2004), The combined Finite-Discrete Element Method, *Wiley.*
- [12] Oñate, E. and J. Rojek (2004), Combination of discrete and finite element method for dynamic analysis of geomechanics problems, *Comput. Methods Appl. Mech. Engrg.* **193**, 3087-3128.
- [13] Wellmann, C. and P. Wriggers (2010), A two-scale model of granular materials, *Comput. Methods. Appl. Mech. Engrg.* **205-208**, 46-58.
- [14] Simo, J.C. and T.J.R. Hughes (1998), Computational Inelasticity, *Springer.*
- [15] Weber, J. (1966), Recherches concernant les contraintes intergranulaires dans les milieux pulvérolents, *Bul. liaison P. et Ch. No. Juillet-août.*
- [16] Radjai, F. and F. Dubois (2011), Discrete modelling of Granular Materials, *John Wiley & Son.*
- [17] Combe, G. and J.-N. Roux (2003), Discrete numerical simulation, a quasistatic deformation and the origin of strain in granular materials, *3rd International Symposium on Deformation Characteristics of Geomaterials*, Lyon-France, 1070-1078.
- [18] Gilabert, F.A., J.-N. Roux and A. Castellanos (2007), Computer simulation of model cohesive powders: Influence of assembling procedure and contact laws on low consolidation states, *Physical Review E* **75**, 011303(1-26).

- [19] Charlier, R. (1987), Approche unifiée de quelques problèmes non linéaires de mécanique des milieux continus par la méthode des éléments finis, *Phd thesis, University of Liège*.
- [20] Desrues J. (1984), La localisation de la déformation dans les matériaux granulaires. Thèse de Doctorat es Science, USMG and INPG, Grenoble, France.
- [21] Desrues, J. and G. Viggiani (2004), Strain localization in sand: an overview of the experimental results obtained in Grenoble using stereophotogrammetry, *Int. J. Numer. Anal. Meth. Geomech.* **28**, 279-321.
- [22] Desrues, J. and R. Chambon (2002), Shear band analysis and shear moduli calibration, *International Journal of Solids and Structures* **39**, 3757-3776.
- [23] Borja, R.I. and J. Wren (1995), Micromechanics of granular media. Part 1: Generation of overall constitutive equation for assemblies of circular disks, *Comput. Methods Appl. Mech. Engrg.* **127**, 13-36.
- [24] Chambon, R., D. Caillerie and T. Matsushima (2001), Plastic continuum with microstructure, local second gradient theories for geomaterials: localization studies, *International Journal of Solids and Structures* **38**, 8503-8527.
- [25] Lagamine code, *University of Liège*.
- [26] Matsushima, T., R. Chambon, D. Caillerie (2002), Large strain finite element analysis of a local second gradient model: application to localization, *Int. J. Numer. Meth. Engrg* **54**, 499-521.
- [27] Nitka, M., G. Combe, C. Dascalu and J. Desrues (2011), Two-scale modelling of granular materials: a DEM-FEM approach, *Granular Matter* **13(3)**, 277-281.